HYDROLOGICAL PROCESSES
Hydrol. Process. **17**, 2521–2539 (2003)
Published online 14 August 2003 in Wiley InterScience (www.interscience.wiley.com). DOI: 10.1002/hyp.1271

Simulating pan-Arctic runoff with a macro-scale terrestrial water balance model

Michael A. Rawlins,[1]* Richard B. Lammers,[1] Steve Frolking,[1,2] Balàzs M. Fekete[1] and Charles J. Vorosmarty[1,2]

[1] *Water Systems Analysis Group, Institute for the Study of Earth, Oceans, and Space, University of New Hampshire, Durham, NH 03824, USA*

[2] *Department of Earth Sciences, University of New Hampshire, Durham, NH 03824, USA*

Abstract:

A terrestrial hydrological model, developed to simulate the high-latitude water cycle, is described, along with comparisons with observed data across the pan-Arctic drainage basin. Gridded fields of plant rooting depth, soil characteristics (texture, organic content), vegetation, and daily time series of precipitation and air temperature provide the primary inputs used to derive simulated runoff at a grid resolution of 25 km across the pan-Arctic. The pan-Arctic water balance model (P/WBM) includes a simple scheme for simulating daily changes in soil frozen and liquid water amounts, with the thaw–freeze model (TFM) driven by air temperature, modelled soil moisture content, and physiographic data. Climate time series (precipitation and air temperature) are from the National Centers for Environmental Prediction (NCEP) reanalysis project for the period 1980–2001.

P/WBM-generated maximum summer active-layer thickness estimates differ from a set of observed data by an average of 12 cm at 27 sites in Alaska, with many of the differences within the variability (1σ) seen in field samples. Simulated long-term annual runoffs are in the range 100 to 400 mm year^{-1}. The highest runoffs are found across northeastern Canada, southern Alaska, and Norway, and lower estimates are noted along the highest latitudes of the terrestrial Arctic in North America and Asia. Good agreement exists between simulated and observed long-term seasonal (winter, spring, summer–fall) runoff to the ten Arctic sea basins ($r = 0{\cdot}84$). Model water budgets are most sensitive to changes in precipitation and air temperature, whereas less affect is noted when other model parameters are altered. Increasing daily precipitation by 25% amplifies annual runoff by 50 to 80% for the largest Arctic drainage basins. Ignoring soil ice by eliminating the TFM sub-model leads to runoffs that are 7 to 27% lower than the control run. The results of these model sensitivity experiments, along with other uncertainties in both observed validation data and model inputs, emphasize the need to develop improved spatial data sets of key geophysical quantities (particularly climate time series) to estimate terrestrial Arctic hydrological budgets better. Copyright © 2003 John Wiley & Sons, Ltd.

KEY WORDS land-surface hydrology; runoff; water balance model; pan-Arctic; active layer

INTRODUCTION

Global-change scenarios have predicted significant positive increases in surface air temperature, with the greatest increases expected to occur in the Arctic (Manabe *et al.*, 1991; Nicholls *et al.*, 1996). Although much speculation surrounds the causes, feedbacks, and uncertainty in Arctic environmental change, a large body of evidence suggests that major changes have already occurred (Serreze *et al.*, 2000; Vörösmarty *et al.*, 2001). Increases in surface air temperature over the next several decades may lead to significant changes in permafrost active-layer thickness (Anisimov *et al.*, 1997). Thawing of permafrost-rich soils can dramatically alter landscape patterns, with a potential to release water and carbon stored in soils (Hinzman and Kane,

* Correspondence to: Michael A. Rawlins, Water Systems Analysis Group, Institute for the Study of Earth, Oceans, and Space, University of New Hampshire, Durham, NH 03824, USA. E-mail: michael.rawlins@unh.edu

Received 31 July 2002
Accepted 8 January 2003

1992; Waelbroeck *et al.*, 1997). Given the linkages between Arctic hydrology and numerous geophysical systems over a wide range of scales, along with recent evidence of significant change (Chapman and Walsh, 1993; Oechel *et al.*, 1993; Groisman *et al.*, 1994; SEARCH SCC, 2001), the mechanisms underlying major hydrological processes across the pan-Arctic deserve considerable attention. Large variations in riverine exports to the Arctic Ocean have the potential to alter global ocean and atmospheric circulations (Broecker, 1997; Schiller *et al.*, 1997), as well as oceanic net carbon storage (Anderson *et al.*, 1998). Major changes in runoff and freshwater export can also affect the biogeochemistry of Arctic aquatic ecosystems (Holmes *et al.*, 2000; Wolheim *et al.*, 2001). And although it contains only 1% of the world's ocean water, the Arctic Ocean receives 11% of the global river runoff (Shiklomanov, 1998).

Models that simulate water budgets at continental and global scales have been widely used in hydrology and Earth science research (Roads *et al.*, 1994; Vörösmarty *et al.*, 1998; Nijssen *et al.*, 2001). Mintz and Walker (1993) applied a simple bucket model to derive global fields of monthly soil moisture. Pitman *et al.* (1999) employed a land-surface model to estimate the effects of frozen soil moisture parameterizations on simulated runoff. A hydrology model was used to evaluate the water budgets of climate model simulations (Maurer *et al.*, 2001), revealing significant biases in the climate model fields. A similar overprediction of evapotranspiration and underprediction of runoff from a climate model land-surface scheme was found across the Yenisei, Lena, and Amur basins in Asia (Arora, 2001). Improvement in global estimates of river discharge were obtained using a new method to determine runoff calibration parameters (Nijssen *et al.*, 2001). Given the lack of observed river discharge data across large portions of the pan-Arctic basin (Lammers *et al.*, 2001; Shiklomanov *et al.*, 2002), hydrological models that adequately capture the Arctic water cycle are needed to provide accurate benchmarks and aid in environmental-change studies. Further, given the significant bias in runoff generated by current general circulation models (Walsh *et al.*, 1998), accurate time series of simulated seasonal runoff routed through a simulated topological network (STN; Vörösmarty *et al.*, 2000a,b) offers the potential to improve freshwater forcing in coupled ocean models.

Thawing and freezing of Arctic soils is affected by many factors, with soil surface temperature, vegetation, and soil moisture among the more significant (Zhang and Stamnes, 1998). Soil texture and slope/aspect also strongly influence active-layer dynamics, which can vary considerably over short lateral distances. Indeed, differences in end-of-season mean thaw depths up to 50% have been found when comparing two sites even in close ($<$10 km) proximity (Nelson *et al.*, 1997).

Investigations of active-layer thickness (ALT) have traditionally been performed through field studies at point locations (Romanovsky and Osterkamp, 1995; Zhang *et al.*, 1996). Given the difficulty in compiling spatially coherent data sets of key input drivers, few studies have been conducted to model seasonal active-layer changes at the regional scale. Anisimov *et al.* (1997) applied a semi-empirical method to calculate the depth of seasonal freezing and thawing using annual air temperature, snow cover, vegetation, soil moisture, and thermal conductivity parameterizations. More complicated models, which simulate heat flow and phase change, have been used to investigate the sensitivity of soil thermal processes to air temperature, seasonal snow cover, and soil moisture (Zhang and Stamnes, 1998). Although detailed models are helpful in understanding the effects of climatic and landscape factors, simple models may be useful in estimating changes in ALT, particularly for large-scale applications. The Stefan solution to the differential equation of heat transfer with phase change under constant conditions (e.g. Lunardini, 1981) shows that ALT progresses as the square root of time. This approach has been applied across the Kuparuk basin (2100 km^2) in northern Alaska (Nelson *et al.*, 1997). Klene *et al.* (2001) found that incorporating the effects of vegetation on soil temperatures could improve this method. In addition to the difficulty in compiling accurate input data sets to model soil thawing and freezing, a lack of empirical observations for validation of simulated estimates presents a further challenge for pan-Arctic applications (Vörösmarty *et al.*, 2001).

Our focus in this paper is the estimation of runoff across the pan-Arctic drainage basin for the period 1980–2001. A simple sub-model for estimating phase changes in soil moisture is described and evaluated by comparing model-estimated ALT with field measurements from several locations in Alaska. Model-simulated runoff is then presented and compared with observed data. The sensitivity of simulated runoff

to variations in climate inputs and model parameterization is also investigated, to identify the most sensitive model requirements.

A PAN-ARCTIC WATER BALANCE MODEL

Large-scale numerical models that simulate the hydrologic cycle have recently been developed to characterize moisture fluxes and storage across diverse landscapes (Nijssen *et al*., 2001; Zhuang *et al*., 2001). Here, we apply a modified version of the water balance model (WBM; Vörösmarty *et al*., 1996, 1998) across the pan-Arctic to study the spatial and temporal variability of the high-latitude terrestrial water cycle, with significant changes incorporated into this version—henceforth referred to as the pan-Arctic water balance model (P/WBM)—detailed in Appendix A.

Models that simulate water and energy balance at fine vertical resolution within the soil have been developed and show promise in estimating soil thermal regimes (Zhuang *et al*., 2001) and water balance (Bruland *et al*., 2001) in Arctic regions. Simple 'bucket' models, however, have been shown to perform comparably to complex biosphere models in estimating soil moisture (Robock *et al*., 1995). A fundamental premise in the development and modification of the P/WBM is that for large-scale spatial applications there are severe limitations in basic data quality needed to parameterize and drive a hydrological model (e.g. precipitation, soil properties, vegetation characteristics, such as leaf area and rooting depth); so, developing a simple, suitably scaled model is appropriate. The model should balance physically based simulations of hydrological processes with the practical limits of soil and vegetation parameterizations and meteorological drivers. To this end, P/WBM is data rich, suitably physically based, and well scaled to the challenges of water budget estimation over the pan-Arctic. Our model does not explicitly simulate glacier accumulation and melt. Therefore, runoff for areas dominated by glaciers and ice fields is expected to have substantial error.

In this study, estimates of snow water equivalent (SWE), soil ice and water stores, along with fluxes such as evaporation, evapotranspiration, and runoff, are made with the P/WBM at explicit daily time steps across the pan-Arctic drainage basin, defined as all land areas draining to the Arctic Ocean in Russia and Canada, as well as Hudson Bay and the Bering Sea (Figure 1). The P/WBM requires spatial data sets of vegetation cover, plant rooting depth, soil texture, soil depth, and soil carbon content. Gridded fields of daily air temperature and precipitation drive the P/WBM. Input data (parameter fields, air temperature, and precipitation) and model output is gridded at 25 km resolution on the Lambert azimuthal equal-area EASE-Grid (NSIDC, 1995; Brodzik and Knowles, 2002). A total of 39 926 EASE-Grid pixels defines the pan-Arctic drainage basin, which extends as far south as 45 °N in southern Canada (Nelson basin) and southern Siberia (Ob basin). Air temperature and precipitation inputs are derived from the National Centers for Environmental Prediction (NCEP) reanalysis project (Kalnay *et al*., 1996; Uppala *et al*., 2000). The NCEP–National Center for Atmospheric Research reanalysis constitutes a retrospective record of numerical weather prediction (NWP) analysis and forecasts, with the added advantage of being constantly updated with minimal (1 month) time lag. Six-hourly NCEP data are aggregated to daily means and interpolated to the 25 km EASE-Grid using a statistical downscaling approach (Serreze *et al*., 2002). Usage of data sets for vegetation cover (Mellilo *et al*., 1993), soil texture (Food and Agriculture Organization/UNESCO, 1995), and rooting depth is based on the methodologies originally reported by Vörösmarty *et al*. (1989). Data for soil organic content were obtained from the Oak Ridge National Laboratory (ORNL) (Global Soil Data Task, 2000).

P/WBM has two soil layers: a root zone that gains water from infiltration and loses water via evapotranspiration and horizontal and vertical drainage, and a deep zone that gains water via root zone vertical drainage and loses water via horizontal drainage (Figure 2). Seasonal changes in soil water/ice content are an important component of Arctic hydrology (Woo, 1998), so specification of phase changes in soil moisture is a key component of the P/WBM. Soil liquid water and ice contents of each soil layer are calculated in a sub-model referred to as the thaw–freeze model (TFM). Because P/WBM does not simulate vertical heterogeneity within either soil layer, it does not explicitly track the depth of thawing or freezing, but instead uses

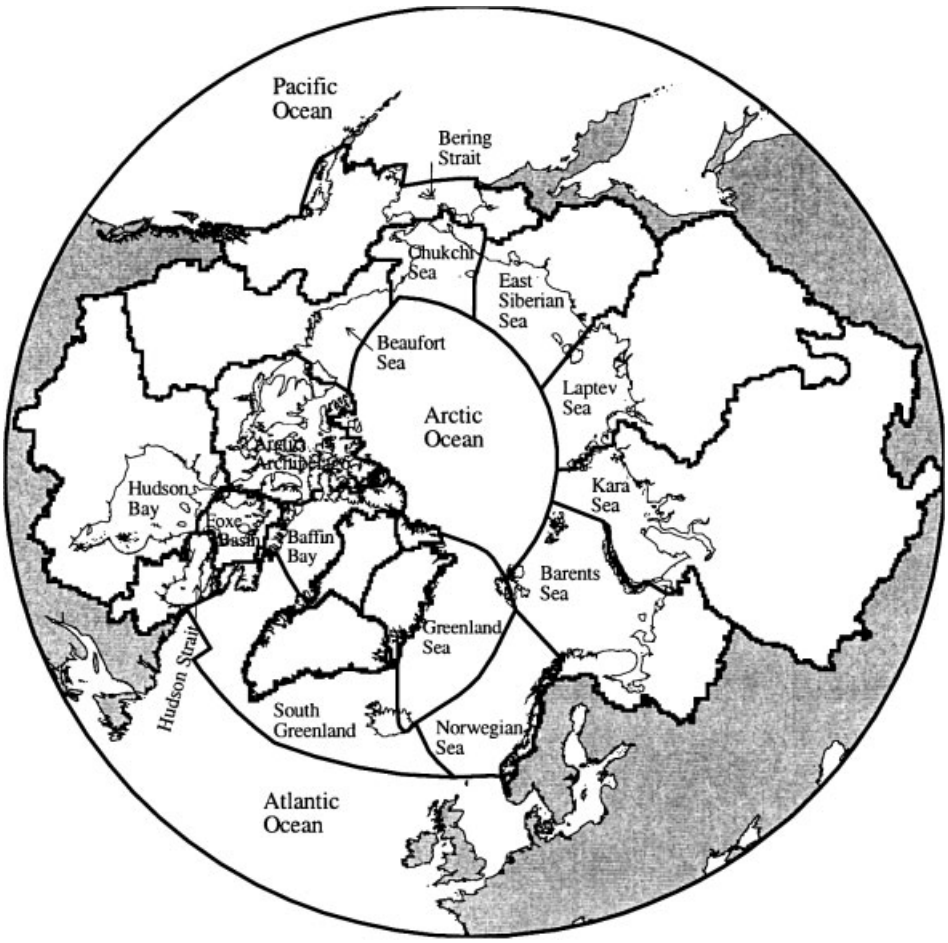

Figure 1. Pan-Arctic domain by sea basin boundaries. Basin boundaries are derived from a digital river network at 30′ grid-cell resolution (Vörösmarty *et al*., 2000a). Shaded region represents areas outside of the pan-Arctic drainage system

the Stefan solution to update daily changes in the amount of liquid and frozen water of each soil layer. The sign of the daily thaw–freeze increment determines the exchange of water and ice within each layer. Details of the TFM are presented in Appendix A.

MODEL RESULTS

Active-layer modelling

To evaluate the efficacy of the Stefan solution, simulated active-layer estimates from the two-layer TFM (Equations (A.4) and (A.5)) within the P/WBM framework are examined. Simulated active-layer development (for a single grid located in northern Alaska) progresses from the organic layer (depth: 23 cm) to mineral soil through the warm season (Figure 3a). Figure 3 also shows the effect of soil moisture variability. After 600 °C-days had accumulated, the ALT for this grid was 38·4 cm for 1999 (drier) and 42·9 cm for 1996 (wetter) conditions, with the variation attributed to differences in thermal conductivity of wet and dry soils. For the purposes of comparison with data in Zhang *et al*. (1997), a linear regression model fit through the estimates in Figure 3a reveals a rate of change approximated by ALT = 0·058 DDT ($r = 0{\cdot}99$), where DDT

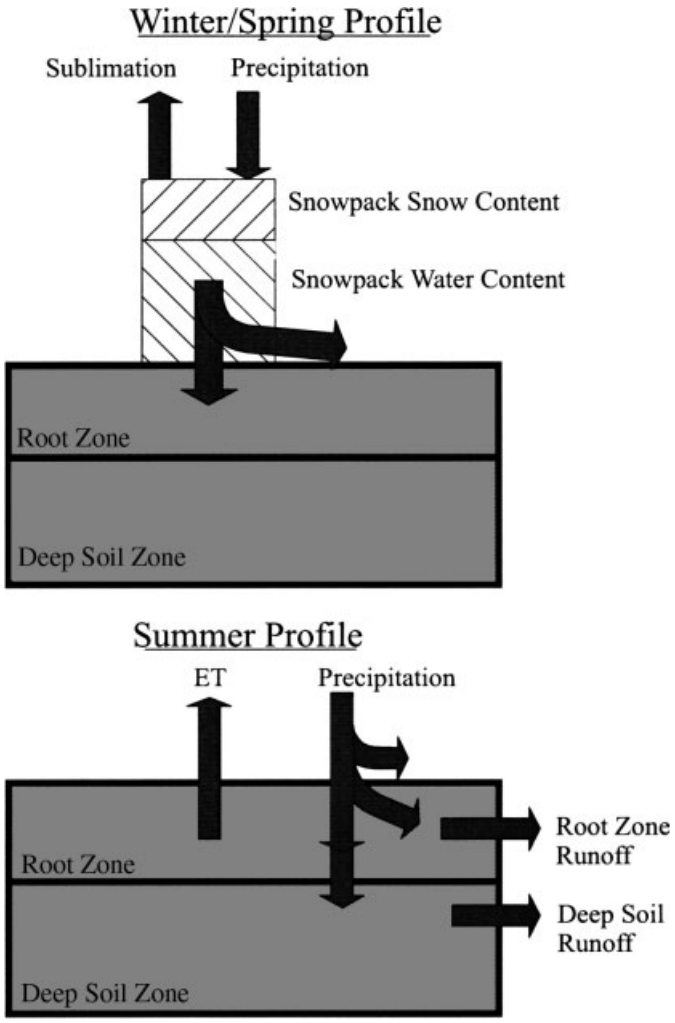

Figure 2. Schematic of the P/WBM soil zones and water fluxes in winter/spring and summer. Root Zone represents the spatially variable vegetation rooting depth. Water in root and deep soil zones can be all frozen, partially frozen, or all liquid. In some locations/cells the deep zone never fully thaws, and in others it never fully freezes (modified from Holden, 1999)

is accumulation of degree days of thawing (°C-day). Zhang *et al*. (1997) examined 17 observations at three locations across northern Alaska (1987–92), and found ALT = 0·046 DDT ($r = 0{\cdot}75$), a difference of 1·2 mm per 10 °C-days from the TFM estimates.

The Stefan solution to heat transfer with phase change in one dimension (vertical) provides a simple estimate of ALT (Lunardini, 1981). Nelson *et al*. (1997) used an empirical ALT similar to the Stefan solution to determine ALT estimates within ~6 cm of observed values. Here, we compare gridded estimates from the two-layer Stefan solution (in the TFM) with a set of observed data from the Circumpolar Active Layer Monitoring network (CALM; Brown *et al*., 2000). Various sampling strategies are represented in the CALM data set, with maximum summer ALT determined as an average of samples across relatively small areas (10 m lattice within a 100 m^2 area), as well as larger sampling designs (100 m lattice within a 1 km^2 area) in some locations. Simulated ALT values on the 25 km EASE-Grid encompassing each CALM validation site are compared with the maximum summer CALM ALT for 27 sites in Alaska (years 1999 and 2000).

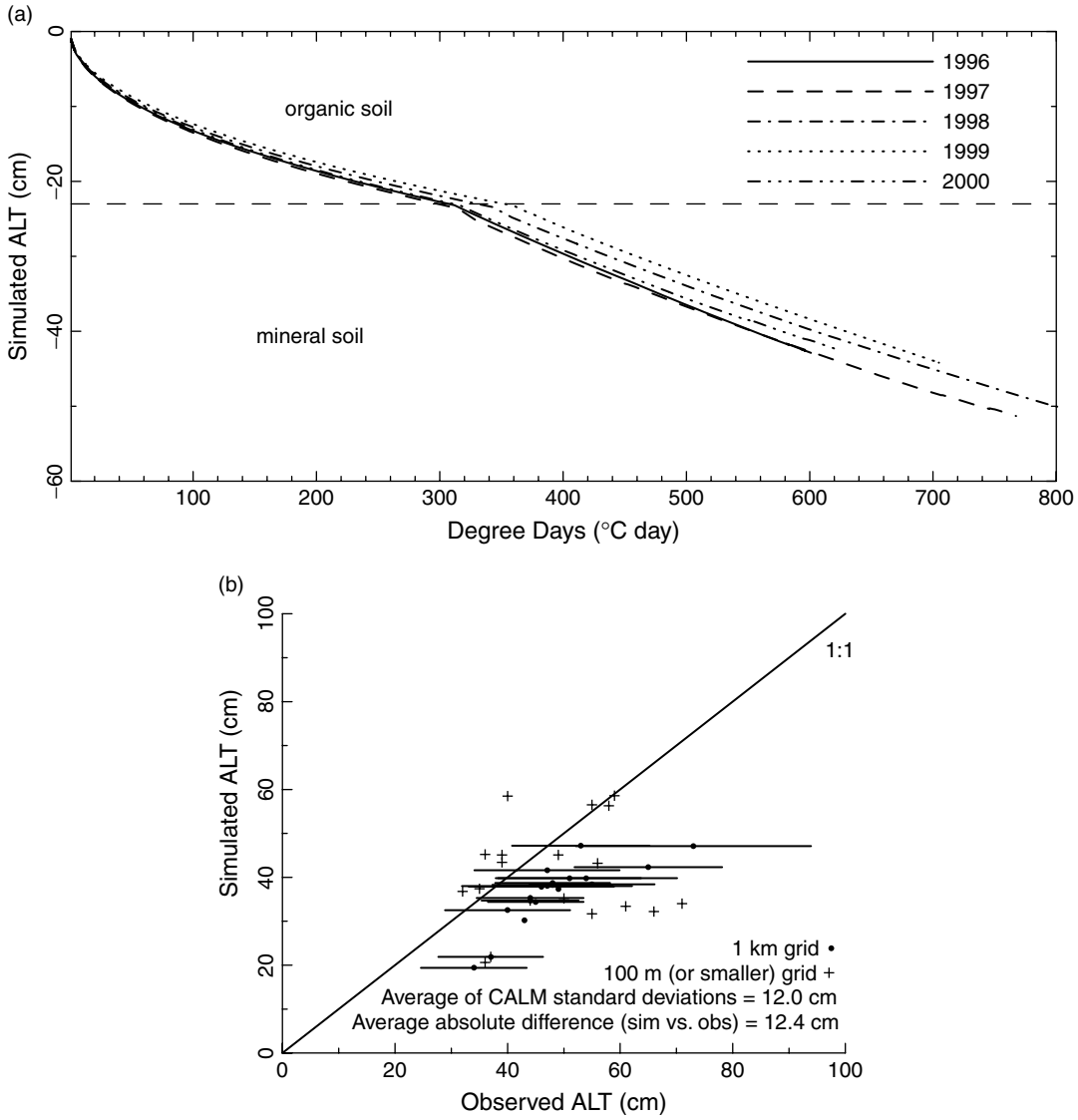

Figure 3. Simulated active layer thickness (ALT) as a function of degree days for one EASE-Grid over North Slope, AK (a); and model predicted active-layer thickness versus CALM observed depth (b). Horizontal lines in lower panel represent one standard deviation on each side of observed ALT for the 1 km^2 CALM sites. The interannual variation in (a) results from differences in soil water content. The 1 km values in (b) are averages of 121 measurements on a 100×100 m^2 grid. Simulated ALT is the P/WBM estimate for the 25 km EASE-Grid cell (625 km^2) encompassing the CALM site

Specifically, we use the TFM model value for the day on which the CALM estimate was made. Model estimates are generally within one standard deviation of the observed value (Figure 3b). A bias (underestimation) in simulated ALT is evident, which is likely attributable, in part, to a bias in the air temperature field that is adjusted to 25 km grid mean elevation, which is higher, and thus cooler, than CALM site elevation in most cases (data not shown). It should be noted that the CALM value used in each comparison represents a single point sample within the 625 km^2 EASE-Grid and grid-to-point comparisons are known to create interpretation problems (Blöschl and Sivapalan, 1995; Vörösmarty *et al*., 1998; Klene *et al*., 2001). And

although an increasing number of CALM sites have begun to employ a gridded sampling design, the use of observed ALT estimates made from a single observation should be undertaken with caution (Brown *et al*., 2000). Nonetheless, the average absolute error of the TFM model versus observations is 12·4 cm (observed data range: 32 to 72 cm), and the average standard deviation of samples from the 1 km^2 grids (100 m lattice) is 12·0 cm. Given the variance in the observed data, TFM estimates are within the variability seen in these field samples. Improvements in ALT estimates using the Stefan solution in this manner have been achieved using higher resolution data sets across the Kuparuk basin in Alaska (Klene *et al*., 2001). Although there is no apparent bias between the comparisons with the 1 km^2 CALM sites and those from smaller areas, there is evidence that the 100 m spacing is unable to resolve the variability in ALT at upland (North Slope, AK) sites (Nelson *et al*., 1999).

Pan-Arctic runoff

To estimate runoff over the pan-Arctic drainage basin, the P/WBM was used to simulate the water cycle at daily time steps for each EASE-Grid across the domain. The model was run with inputs of air temperature and precipitation for the year 1980, repeated for 50 years to stabilize soil moisture content, followed by a transient run for the years 1980–2001. Climatologies of monthly total runoff (Figure 4) show the progression of the annual pattern of runoff, from the spring snowmelt pulse, to low-flow conditions, to freeze-up. Monthly runoff is relatively low across much of the terrestrial Arctic in winter, with the exception of coastal western Canada and southern Alaska. Snowmelt contributes to higher runoff across Eurasia in April. Runoff increases in both magnitude and extent during May in both hemispheres. The most northern areas of Eurasia see the snowmelt-driven runoff peak in June. In a general sense, this peak runoff progresses northward toward the Arctic Ocean through spring in central Eurasia, indicative of seasonal changes in surface air temperature. Summer rainfall then contributes to runoff through summer; however, higher evapotranspiration tends to produce relatively dry conditions. The water cycle in fall and winter is dominated by snowpack accumulation and low runoff amounts.

Simulated long-term annual runoff (1980–2001) is highest across southern Alaska, coastal Norway, and Iceland. Higher runoffs are also found across southern parts of Canada in the Nelson basin and the Eurasian part of Russia. Lower runoffs are evident across the Canadian archipelago and Siberia (Figure 5). Runoffs exceeding 400 mm $year^{-1}$ are noted across northeastern Canada and southern Alaska. Simulated long-term annual runoff across the largest Arctic drainage basins is approximately 100 to 180 mm $year^{-1}$ (Table I). More variability, however, is seen in runoff to individual Arctic sea basins; runoff ranges from 90 mm $year^{-1}$ (East Siberian Sea, Table I) to as much as 300 mm $year^{-1}$ (Hudson Strait).

Spatially averaged simulated runoff is approximately 180 mm $year^{-1}$ across the entire pan-Arctic drainage basin. Simulated annual runoff is approximately 40–70% of the annual downscaled precipitation (Serreze *et al*., 2002) across many regions and is highly correlated with precipitation ($r = 0{\cdot}90$). Higher variability in observed runoff is apparent (Figure 6), and the correlation with precipitation is lower ($r = 0{\cdot}56$). Observed runoff is generated by distributing a basin's discharge across the monitored region, including areas between gauging stations (inter-station areas) (Lammers *et al*., 2002). Observed discharge estimates for the period 1980–97 are from a data set of 650 gauging stations across the pan-Arctic (Lammers *et al*., 2001; Shiklomanov *et al*., 2002). Discrepancies due to the use of different averaging periods (simulated runoff from 1980 to 2001, observed from 1980 to 1997) are assumed to be negligible. Mean values of the simulated and observed runoff distributions for precipitation between 300 and 900 mm (80% of total samples) are comparable (Figure 6). P/WBM-simulated runoff is conservative (does not exceed precipitation) and the residual of precipitation minus runoff represents modelled evapotranspiration. Observed runoff, however, exceeds the inter-station-area precipitation in some regions, implying either considerable interbasin groundwater transfers or significant problems with the spatial precipitation and/or runoff data (Vörösmarty *et al*., 1998; Fekete *et al*., 1999).

Simulated and observed runoffs are further compared by aggregating to long-term seasonal runoff for each Arctic sea basin. Seasonal runoff represents the total stock of freshwater that contributes to the sea basin's seasonal riverine input. Here, we compare the integrated runoff across all EASE grids in a given basin with the

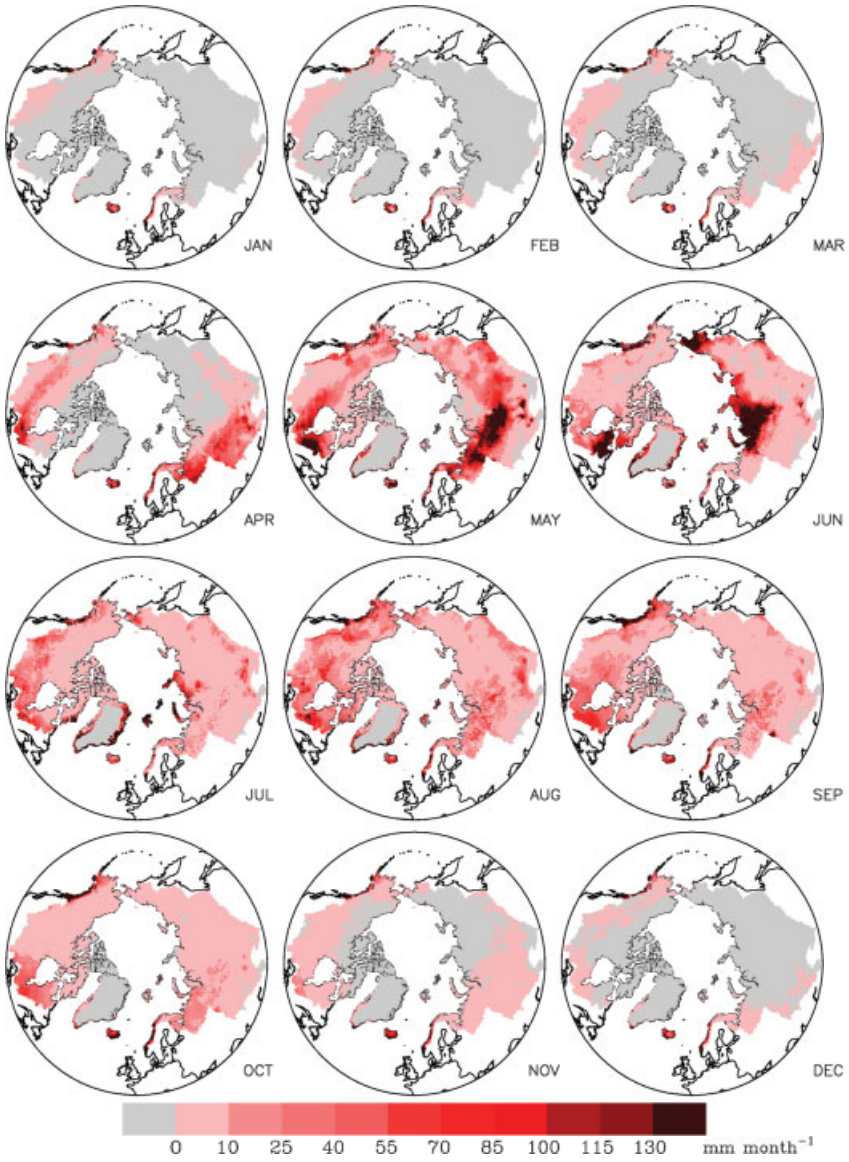

Figure 4. P/WBM long-term monthly runoff climatology 1980–2001. This figure includes runoff for southern Alaska, which is not part of the pan-Arctic drainage *per se*. Grids with zero runoff for the month are shaded in gray. Runoff for areas with glaciers should be interpreted with caution, as the P/WBM does not model glacier accumulation and melt/ablation

observed runoff over the monitored portion of that basin. Although underestimates are again more common than overestimates, good correlation is evident ($r = 0{\cdot}84$, Figure 7). The P/WBM runoff estimates are near zero in winter, and underestimate most observed basin values. This is likely due to several factors, including groundwater inputs that do not freeze in winter, and lags in water transport that generate winter flow (observed at gauging stations) from fall runoff. For some basins, the monitored area is only a small fraction of the total basin (Table I), which could introduce a bias into the observed runoff, evidence that the decline in river discharge monitoring across both North America and Asia (Shiklomanov *et al.*, 2002) complicates our model verification efforts.

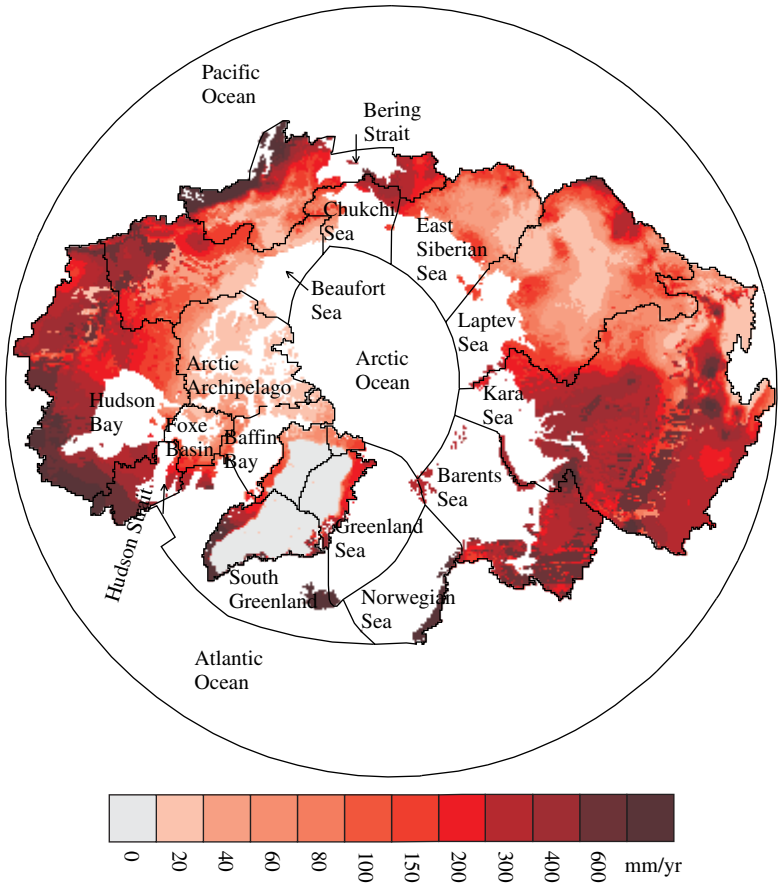

Figure 5. P/WBM simulated annual long-term mean runoff for years 1980–2001 across the 25×10^6 km^2 land area of the pan-Arctic drainage basin. Annual runoff is estimated at the 39 926 EASE-Grids (equal area 25 km × 25 km) defining the domain. This figure includes runoff for southern Alaska, which is not part of the pan-Arctic drainage. Grids with zero annual runoff are shaded in blue. Runoff for areas with glaciers should be interpreted with caution, as the P/WBM does not model glacier accumulation and melt/ablation

SENSITIVITY ANALYSIS

Biogeophysical characteristics, such as plant rooting depth, organic-layer thickness, and soil texture, affect water flow paths and are integral factors in hydrological models. In addition, climate data (precipitation and air temperature) are essential inputs, with both spatial and temporal variations and uncertainties. Precipitation and air temperature data for the Arctic, however, are more poorly resolved (owing to the sparsity of meteorological stations), relative to other parts of the world. In addition to being undersampled, biases in Arctic precipitation records are known to be large, particularly at higher latitudes. Underestimates of 20–25% (Karl *et al*., 1993) and 10–140% (Yang *et al*., 1998) have been determined across North America and at ten locations in Alaska respectively. Substantial gauge undercatch across the Arctic has also been estimated by applying a hydrological model (Fekete *et al*., 1999). Although NCEP reanalysis data have been adjusted for measurement biases (Serreze *et al*., 2002), some uncertainty in the model input can be assumed. Comparison of daily gridded NCEP air temperatures in summer with observed meteorological data yielded absolute differences from 1.6 °C for an Arctic continental location and 6.6 °C at a coastal site. In general, NCEP air temperatures are consistently cooler than the station observations throughout summer.

Table I. Simulated long-term annual runoff for selected Arctic drainage basins and terrestrial runoff integrated across basins draining to selected Arctic Ocean sea basins

Basin	Basin size/ contributing area[a] (km^2)	Gauged area[b] (km^2)	Simulated annual runoff (mm $year^{-1}$)
River basin	*Basin Size*[a] (Km^2)		
Ob	2 994 238	2 965 100	180
Yenisei	2 537 404	2 452 300	170
Lena	2 460 742	2 460 000	100
Mackenzie	1 783 972	1 769 200	150
Yukon	833 232	831 391	120
Nelson	1 106 578	1 050 300	160
Sea basin	*Contributing Area*[a] (Km^2)		
Arctic Archipelago	1 134 856	209 270	40
Hudson Bay	3 304 025	2 613 320	270
Barents Sea	1 322 741	984 830	300
Hudson Strait	468 050	285 480	410
Beaufort Sea	2 139 635	1 860 100	130
South Greenland	1 174 444	10 800	250
Bering Strait	1 205 234	1 010 940	170
Kara Sea	6 631 308	5 159 700	200
Chukchi Sea	282 143	56 160	190
Laptev Sea	3 639 584	3 232 480	100
East Siberian Sea	1 329 025	941 500	90
pan-Arctic[c]	22 611 659	16 460 080	180

[a] Total area for river or sea basin on the EASE-Grid (NSIDC, 1995).
[b] Area captured by observed gauging stations (Lammers *et al*., 2001).
[c] Annual runoffs in Table represent an integration across all EASE grids in a given basin.
[d] The Pan-Arctic value represents the spatially-averaged runoff for all land areas draining to the Arctic Ocean in Russia, Canada and Alaska, as well as Hudson Bay and the Northern Bering Sea. Runoff from basins dominated by glaciers should be interpreted with caution, as the P/WBM does not model glacier accumulation and melt/ablation.

To investigate the sensitivity of the P/WBM to model parameterizations and climate inputs, long-term annual runoff (1980–2001) was compared against the long-term annual runoff produced in a series of model perturbations runs. The following perturbation experiments were performed: (i) model organic-layer depths were halved [0·5 × Org] and (ii) doubled [2 × Org]; (iii) vegetation rooting depths were halved [0·5 × RD] and (iv) doubled [2 × RD]; (v) soil field capacity was increased by 0·05 cm^3 cm^{-3} of pore space [FC + 25%]; (vi) horizontal and downward water flux from rooting zone (Figure 2) was increased to 40% (from 20%) of water over field capacity [RF = 40%]; (vii) the TFM sub-model was not applied [No TFM]; (viii) summer air temperatures were increased by 4 °C [T + 4 °C] and (ix) daily precipitation was increased by 25% [P + 25%]. The control run represents our best estimate of annual runoff, e.g. Figure 5 (with associated error characteristics as discussed above), using available fields of soil characteristics, NCEP-derived air temperature and precipitation, and the TFM-generated active-layer behaviour. Comparisons were examined for the Yukon, Nelson, MacKenzie, Ob, Yenisei, and Lena River basins. Differences between the control and sensitivity runs were also determined for the entire pan-Arctic basin.

Of the nine sensitivity experiments performed, an increase in precipitation produces the most significant changes in basin-average runoff. Adding 25% to each daily precipitation occurrence increases Arctic-wide and basin runoff well over 50% (Figure 8), as additional precipitation is more likely to be diverted to runoff than evapotranspiration. Bias in precipitation inputs has been noted as a primary source of error in other large-scale hydrology models (Nijssen *et al*., 2001).

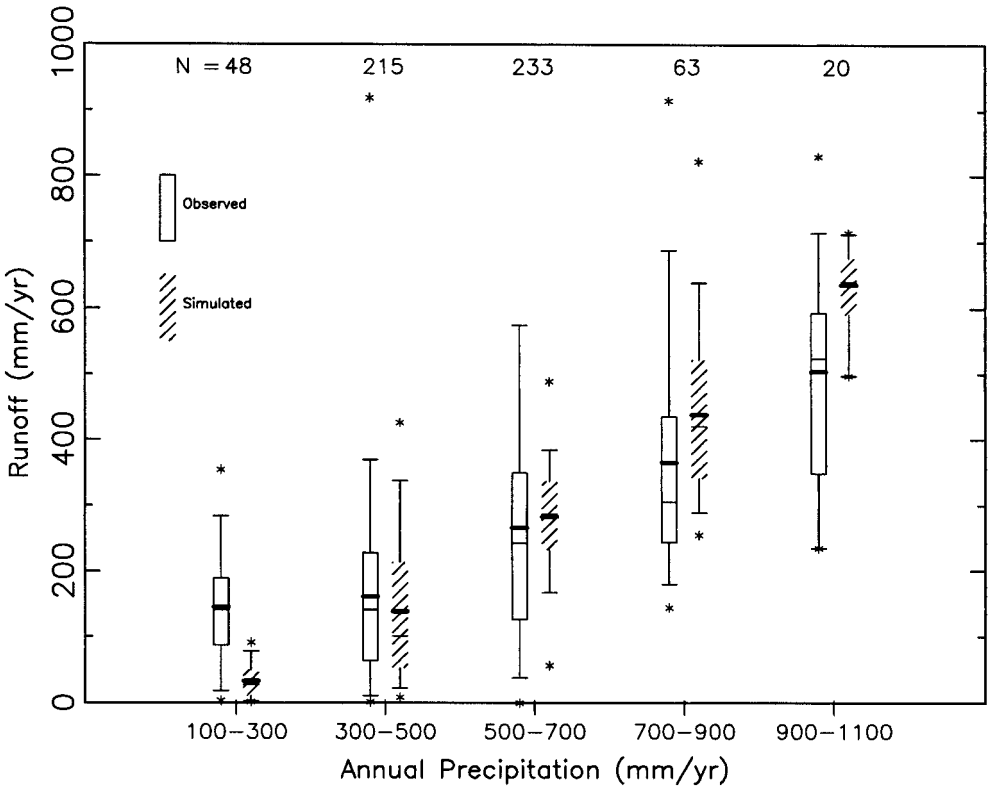

Figure 6. Distribution of simulated and observed annual (long-term) runoff at ($n = 579$) inter-station areas for groupings of annual long-term precipitation. The top and bottom of each box are the 25th and 75th percentiles respectively. Boxplot whiskers represent the 5th and 95th percentiles. The spatial mean is the thick line and the median is the thin line. Maximum and minimum runoff for each distribution is marked with an asterisk. The number of observed and simulated runoffs in each grouping is listed along the top of the figure. Maximum value of observed runoff for 500–700 precipitation is 1915 mm and is not plotted. Note that in all bins, except 900–1100 mm year^{-1}, the maximum observed runoff is greater than annual precipitation

Increasing the daily summer air temperatures by 4 °C also has a significant effect (albeit smaller than precipitation) across much of the pan-Arctic. Annual runoff is reduced by more than 20% across the Yukon, Lena, and Nelson basins (Figure 8). Warmer air temperatures result in higher rates of evapotranspiration (Equation (A.1)), enhanced development of the active layer each spring/summer, an increased water-holding capacity (which allows for more evapotranspiration) and, therefore, less runoff. The larger changes across the Yukon and Lena basins are expected, considering the greater extent of permafrost conditions in these areas relative to the other basins. A similar mechanism and magnitude of effect occurs when the TFM sub-model is not used, effectively neglecting the seasonal thawing and freezing (i.e. changes to water-holding capacity) of Arctic soils. In this case, the absence of a shallow active-layer in late spring and early summer results in higher infiltration and summer evaporation, with a resultant reduction in annual runoff of 7% for the Yenisei basin (least effect) to 27% for the Yukon basin (greatest effect). This result is consistent with a recent investigation of soil frost effects on catchment runoff, which found that ignoring soil frost tends to decrease total runoff (Stähli *et al.*, 2001). However, two recent studies have questioned the importance of modelling soil ice for runoff estimation in forested environs (Nyberg *et al.*, 2001) and at large basin scales (Pitman *et al.*, 1999).

As opposed to the perturbations to climate inputs (and the TFM), changes to other model parameterizations result in relatively smaller changes (generally <15%) in annual runoff. Reducing organic layer depths enhances active-layer development, reducing runoff (Figure 8). A doubling of rooting depths (as well as an increase in

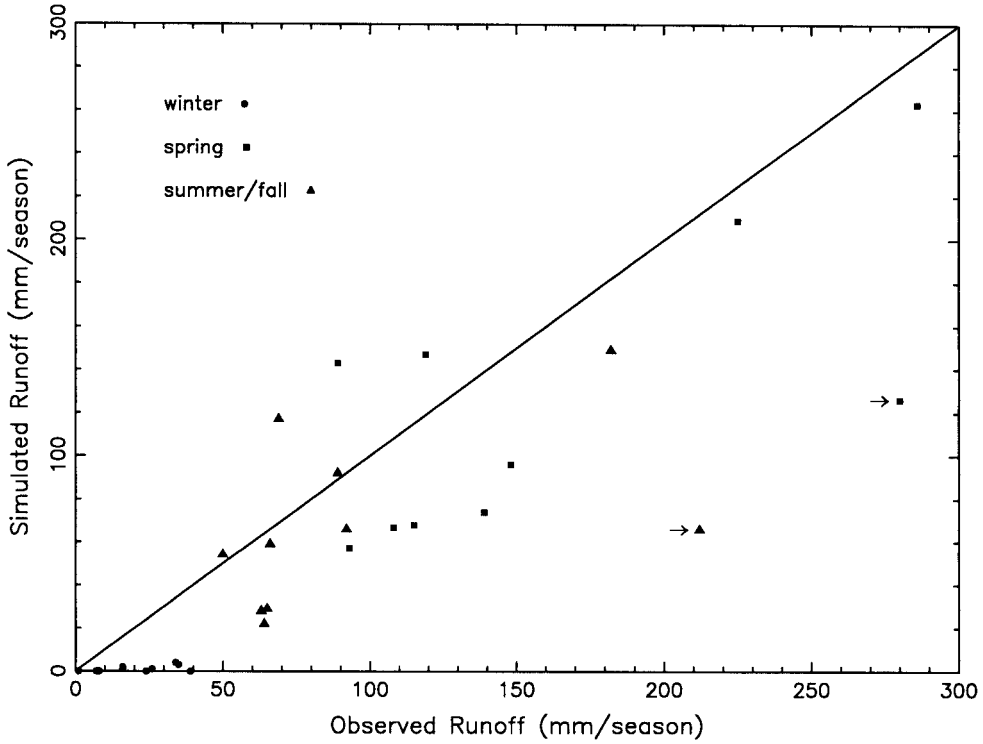

Figure 7. Long-term seasonal runoff at Arctic sea basins. Winter is December, January, February, March; spring is April, May, June, July; summer–fall is August, September, October, November. Note: the observed Chukchi Sea values for spring and summer–fall (labelled with →) are based on only a few gauges, and any results relating to these observations will be more sensitive to temporal changes in the representative gauge(s). Observed runoff values are taken from Lammers *et al.* (2001)

field capacity) also increases soil water-holding capacity, which lowers runoff. Runoff changes are negligible when the flux from the rooting zone is increased. These differences from the control runoff are significantly less than the standard deviation in annual runoff, further emphasizing the relatively small impact of these model parameterizations compared with the climate inputs.

SUMMARY AND CONCLUSIONS

A comprehensive understanding of Arctic hydrological systems has become important in light of recent evidence of the region's environmental changes. Given the linkages involving water and carbon in terrestrial landscapes, the atmosphere and oceans, quantifying the Arctic water cycle at continental scales allows us to establish baseline conditions and explore changes predicted to occur (SEARCH SCC, 2001). River discharge is highly undersampled across many of the higher latitudes in the pan-Arctic drainage basin. With recent closures to a number of observed discharge monitoring stations (Shiklomanov *et al.*, 2002), modelling efforts that simulate runoff and freshwater flux to the Arctic Ocean can provide the requisite inputs to ocean models in lieu of observed data.

The P/WBM has been developed and applied to estimate the water cycle at daily time steps for the 25×10^6 km^2 land area of the pan-Arctic drainage basin for the period 1980–2001. Phase changes in soil moisture were simulated with the TFM. These linked models utilize spatial fields of vegetation rooting depth, organic-layer depth, and soil textures, and are driven with climate data from the NCEP reanalysis project. These spatial data sets are of varying quality, and many regions are severely undersampled in all variables.

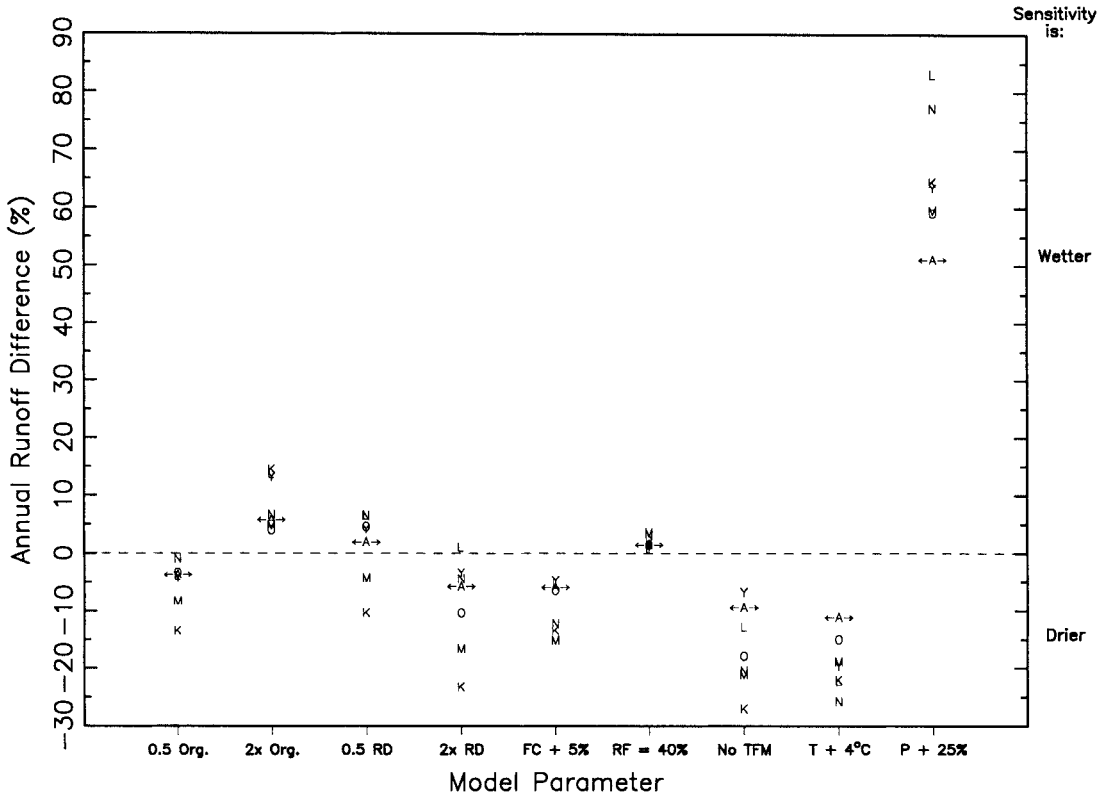

Figure 8. Sensitivity of simulated annual runoff climatology to various alterations of input parameters. Relative percent differences are defined by $\Delta RO = (RO_c - RO_p)/RO_c \times 100\%$ where ΔRO is the relative difference in percent, RO_c is the 1980–2001 runoff climatology, and RO_p is the 1980–2001 runoff climatology for perturbation or sensitivity run. Basins in analysis are O = Ob, Y = Yenisei, L = Lena, M = Mackenzie, N = Nelson, K = Yukon, ←A→= pan-Arctic. Perturbation experiments are as follows: model organic-layer depths are halved [0·5 × Org], doubled [2 × Org], vegetation rooting depths are halved [0.5× RD], and doubled [2 × RD], soil field capacity is increased by 0·05 cm^3 cm^{-3} of pore space [FC + 25%], horizontal and downward water flux from rooting zone is increased to 40% (from 20%) [RF = 40%], TFM sub-model is not applied [No TFM], summer air temperatures are increased by 4° [T + 4 °C], and daily precipitation is increased by 25% [P + 25%]

Nonetheless, their compilation and analysis in the context of water balance models provides one framework for evaluating consistencies between data sets (e.g. runoff and precipitation), as well as providing a means for simulating the hydrological cycle.

ALT generated with the TFM were compared with observed data from the CALM network. Simulated end-of-season ALT was generally within the range of variability seen in the observed data; model biases were 12·4 cm, and the average standard deviation of the observed CALM estimates is 12·0 cm. In large-scale studies of this nature, the observed data validation sites, even 1 km^2 grid sampling, represent point estimates within the larger (625 km^2) P/WBM grid. Considerable variability exists at this scale in all biophysical parameters, including seasonal *n*-factors, with soil-surface degree-day sums varying up to 100% within 1 ha plots (Klene *et al.*, 2001). Although simulated maximum summer ALT estimates are generally within the variability observed in the field samples, our interest centres on the day-to-day changes in active-layer development used to determine phase changes of soil water. Recent studies (Anisimov *et al.*, 1997; Klene *et al.*, 2001) have suggested that improvements in active-layer simulation are dependent on the development of more spatially coherent data sets of air temperature, vegetation, and soil moisture.

Simulated monthly runoff is relatively low during winter, when precipitation accumulates as snow. A spring melt pulse is evident in a south-to-north progression across the Arctic basin, with the majority of

runoff occurring between the months of April and June. Annual long-term runoff is highest across coastal western Canada, northeastern Canada and west central Eurasia. Lowest annual runoffs are seen across the Canadian archipelago and Siberia. Simulated long-term annual runoff is less variable than observed runoff, and is highly correlated with precipitation. Good correspondence was found when comparing simulated and observed seasonal runoff at individual Arctic sea basins ($r = 0{\cdot}84$). This suggests that the P/WBM has the potential to provide the seasonal (temporal) variations in freshwater discharge to ocean circulation models. Our sensitivity analyses show this model to be strongly influenced by climate drivers, as well as by the absence or presence of modeled active-layer changes, and that uncertainties in parameters such as rooting depth and organic layer thickness may be less problematic. We believe that, as important as model development is, it is essential for the research community to work to improve spatial data sets for fundamental biophysical variables and climatic drivers, and to maintain and expand river gauging in the pan-Arctic to provide more complete data sets for model evaluation. Simulation of the Arctic water cycle is moderately influenced by specification of active-layer changes. This finding suggests that modelling and analyses that depend on hydrological drivers, such as ocean circulation, coastal processes, ecosystem biogeochemistry, and climate models, will benefit from incorporation of thawing and freezing of Arctic soils. The gridded runoff fields presented here are available from the Water Systems Analysis Group, University of New Hampshire, USA.

ACKNOWLEDGEMENTS

We would like to thank Anthony Federer, and Alexander Shiklomanov (UNH) for their generous input to this research, and Mark Serreze (National Snow and Ice Data Center) for supplying the climate inputs. Jonathan Holden helped in developing an earlier version of the P/WBM. Stanley Glidden is thanked for his programming assistance. This research was supported by: the NSF ARCSS program and NSF grants OPP-9818199, OPP-9910264, and OPP-0094532; NASA grants NAG5-9617, NAG5-6137, NAG5-11256, and NAG5-11750 and US Department of Defense grant N00014-01-1-0357.

APPENDIX A

The P/WBM is a daily explicit hydrologic model, whereas the WBM contains an optimized soil moisture routine and is run using monthly inputs and a quasi-daily, statistically equivalent daily time step (Vörösmarty *et al*., 1998). The significant changes to the original algorithms that comprise the P/WBM are described below.

Snow dynamics

Daily precipitation for each grid is partitioned into either rain or snow based on a daily air temperature threshold of 0 °C. The simulated snowpack contains both a solid (frozen) and liquid portion, providing a total model value for SWE. Sublimation from the frozen snow is determined through a simple function (Hamon, 1963), which allows for a small amount of sublimation at air temperatures below freezing. The function is

$$E_t = 715{\cdot}5\Lambda e(T_t)/(T_t + 273{\cdot}2) \tag{A.1}$$

where E_t (mm day^{-1}) is sublimation (or potential evapotranspiration when snow is absent), Λ is daylength (fraction of day), and $e(T_t)$ (kPa) is daily saturated vapour pressure at temperature T_t (°C).

Daily snowmelt, a function of rainfall and/or air temperature, is

$$M_t = f_{\mathrm{v}}(2{\cdot}63 + 2{\cdot}55T_{\mathrm{t}} + 0{\cdot}0912T_{\mathrm{t}}P_{\mathrm{t}}) \tag{A.2}$$

where M_t (mm day^{-1}) is snowmelt f_{v}, (dimensionless, range 0·4 to 1·0) is a vegetation factor that accounts for the differential absorption of radiation for different landcover types (Federer and Lash, 1978), T_{t} (°C)

represents daily air temperature and P_t (mm day^{-1}) is precipitation, all on day t (Willmott *et al.*, 1985). Snowmelt and/or rainfall contributes to the liquid portion of the snowpack. Damming of snowmelt runoff is a complex process that delays the timing of streamflow during spring (Hinzman and Kane, 1991). In the P/WBM, the snowpack is assumed to retain liquid water until this liquid content exceeds 80% of the snowpack frozen portion's water equivalent (SWE_t), whereupon a fraction (60%) of the snowpack liquid water is released to the soil surface. The value of 80% represents all processes of delay to release of liquid water within the 625 km^2 grid cell. This process is determined through

$$\mathrm{AW}_t = \begin{cases} \mathrm{SW}_t\gamma, & \mathrm{SW}_t \geq \sigma\mathrm{SWE}_t \\ 0 & \text{otherwise} \end{cases} \tag{A.3}$$

where AW_t (mm day^{-1}) is water made available to the soil surface, SW_t (mm) is the snowpack liquid water content, SWE_t (mm) is snowpack frozen water content, γ is the percentage of SW_t released from snowpack (0·6 or 60% day^{-1}), and σ is the critical threshold (80%).

Soil sub-model

Daily changes in the P/WBM soil liquid water and ice content are made by using gridded fields of soil properties and daily air temperature and the Stefan solution to heat transfer with phase change in a uniform semi-infinite medium (Lunardini, 1981), defined by

$$z(t) = \sqrt{\frac{2k(n\mathrm{DDT}(t))}{w\rho L}} \tag{A.4}$$

where $z(t)$ (m) is the depth of the phase change boundary, k (J m^{-1} °C^{-1} day^{-1}) is the soil thermal conductivity above the phase-change boundary, n (dimensionless) is the n-factor, relating integrated air temperature to integrated soil-surface temperature (Lunardini, 1978), DDT(t) (°C-day) is the accumulated degree days of thaw (or freeze), w (kg kg^{-1} dry soil) is the soil water content at the phase-change boundary, ρ (kg m^{-3}) is the soil bulk density, and L (J kg^{-1}) is the latent heat of fusion of water. Our implementation of Equation (A.4) within the TFM includes an assumption of saturation at the interface between thawed and frozen soils. Although used frequently in engineering applications involving paved surfaces, few scientific studies have estimated spatially variable n-factors across large areas. A constant value of 0.8 was assigned for all EASE-Grids, which represents an average n-factor across several vegetative classes determined using multiple observations of air and soil-surface temperatures at sites in northern Alaska (Klene *et al.*, 2001).

Organic soils have very different thermal properties than mineral soils (van Wijk and de Vries, 1963), and since many soils in the pan-Arctic have a surface organic layer, we used the two-layered-soil Stefan solution (Jumikis, 1997). If the freeze–thaw depth calculation is within the surface layer, Equation (A.4) applies with organic soil thermal properties (k_o, w_o, and ρ_o), otherwise the depth is given (after Jumikis (1977)) by

$$z(t) = z_o\left(1 - \frac{k_m}{k_o}\right) + \sqrt{\left(z_o\frac{k_m}{k_o}\right)^2 - \left(z_o^2\frac{k_m w_o \rho_o}{k_o w_m \rho_m}\right) - \frac{2k_m n\mathrm{DDT}(t)}{w_m\rho_m L}} \tag{A.5}$$

where the subscript 'o' refers to organic soil properties and the subscript 'm' refers to mineral soil properties. Soil thermal conductivity for organic (k_o, J m^{-1} °C^{-1} day^{-1}) and mineral (k_m, J m^{-1} °C^{-1} day^{-1}) soils is a function of soil moisture and soil texture (Table II). Organic-layer thickness was estimated by assuming half of the total soil organic matter (Global Soil Data Task, 2000) is in the surface organic layer, with a bulk density of 100 kg m^{-3}. Organic-layer thicknesses across the pan-Arctic range from 0·10 to 0·70 m, with a pan-Arctic mean of 0·22 m.

Daily soil conductivity (k_o and k_m) for each grid cell is obtained by using the P/WBM-generated soil moisture and linearly interpolating between conductivity associated with two of the three moisture classes: dry (soil moisture ~0%), wet (50%) and saturated (100%) (Table II).

Table II. P/WBM soil texture classes and model parameters

Texture	Porosity ($cm^3\ cm^{-3}$)	Field capacity ($cm^3\ cm^{-3}$)	Wilting point ($cm^3\ cm^{-3}$)	Bulk density ($g\ cm^3$)	Thermal conductivity (Saturated, Wet, Dry)[a] ($cal\ cm^{-1}\ s^{-1}\ °C^{-1}$)
Coarse	0·39	0·05	0·04	1·6	5·2, 4·2, 0·7
Coarse + medium	0·43	0·14	0·05	1·5	4·8, 3·8, 0·7
Medium	0·45	0·24	0·09	1·44	4·3, 3·3, 0·6
Coarse + fine	0·45	0·24	0·09	1·44	4·3, 3·3, 0·6
Coarse + medium + fine	0·45	0·24	0·09	1·44	4·3, 3·3, 0·6
Medium + fine	0·48	0·32	0·17	1·35	3·9, 2·9, 0·6
Fine	0·53	0·35	0·22	1·21	3·8, 2·8, 0·6
Organic	0·92	0·5	0·1	0·1	1·2, 0·7, 0·14

[a] Data from Van Wijk and de Vries (1963).

Soil moisture (water and ice) is determined from interactions between the changing active-layer thickness, snowmelt and/or rainfall, and evapotranspiration. Runoff occurs when (i) soil moisture exceeds field capacity or (ii) snowmelt and/or rainfall exceeds a predefined critical value (described below). Whereas changes in soil water content have a significant effect on ALT, variations in seasonal snow cover have a relatively slight impact (Zhang and Stamnes, 1998). The P/WBM accounts for the insulating effects of snowcover through a delay to soil thawing in spring when model snow cover is present.

Change in ALT is used to determine the amount of water that changes phase (melt or freeze) on a daily basis. Soil ice (water) that melts (freezes) is also dependent on the relative saturation of the zone. The amount of ice that melts (freezes) is thus

$$L_t = \Delta z_t R_t \tag{A.6}$$

where L_t (mm day^{-1}) is melt (freeze) on day t, Δz_t (mm day^{-1}) is the increase (decrease) in ALT on day t, and R_t is the relative saturation of the zone (0 to 1). Relative saturation is defined

$$R_t = \frac{I_{t-1} + W_{t-1}}{\mathrm{SD}} \tag{A.7}$$

where I_{t-1} (mm) is soil ice and W_{t-1} (mm) is soil water, both from the previous day, and SD (mm) is the total pore space of the soil layer. If $\Delta z_t > 0$, then ice is melted. Liquid water is converted to ice when $\Delta z_t < 0$. If $\Delta z_t = 0$, then there is no water phase change. This algorithm is used to change the phase of water in the deep soil layer when all water has been converted in the overlying root zone.

Daily snow drainage and/or rainfall infiltrates the root zone to recharge soil moisture storage to a maximum of 12 mm day^{-1}. Surface inputs (snow drainage and rain) greater than this threshold contribute to runoff. Soil recharge is defined

$$R_{\mathrm{w}} = \mathrm{IW} F_{\mathrm{w}} \frac{W}{W + I} \tag{A.8}$$

where R_{w} (mm day^{-1}) is recharge to the soil reservoir of water, IW (mm day^{-1}) represents water infiltrating the soil, W (mm) is root zone soil water, and I (mm) is root zone ice content. The remaining fraction of infiltration water contributes to soil ice storage.

The upper soil (root) zone loses water through evapotranspiration, lateral movement, and vertical drainage to the deep soil zone. Potential evapotranspiration (PE) is estimated with the Hamon function (Hamon, 1963) (Equation (A.1)). Vegetation is assumed to utilize soil moisture at the potential rate when soil water is greater than or equal to field capacity. In times of moisture stress, evapotranspiration is a fraction of the potential

rate, and is determined through a soil-retention function (Vörösmarty *et al*., 1989). The field capacity for each layer is

$$FC_r = (SD_r - I_r)\alpha \tag{A.9}$$

where FC_r (mm) is field capacity in the root zone, SD_r (mm) is pore space, I_r (mm) is ice content, and α (%) is field capacity (Table II). Water draining vertically is proportioned into liquid water and ice in the deep zone

$$d_w = B\frac{W_d}{W_d + W_i} \tag{A.10}$$

where d_w (mm) is the vertical flux per day that contributes to water in the deep zone, B (mm) is the excess water from the root zone, W_d (mm) is water in the deep zone, and W_i (mm) is ice in the deep zone. The contribution to deep zone ice d_i (mm) is

$$d_i = B\frac{W_i}{W_d + W_i} \tag{A.11}$$

REFERENCES

Anderson LG, Olsson K, Chieriei M. 1998. A carbon budget for the Arctic Ocean. *Global Biogeochemical Cycles* **12**: 455–465.

Anisimov OA, Shiklomanov NI, Nelson FE. 1997. Effects of global warming on permafrost and active-layer thickness: results from transient general circulation models. *Global and Planetary Change* **15**: 61–77.

Arora VK. 2001. Assessment of simulated water balance for continental-scale river basins in an AMIP 2 simulation. *Journal of Geophysical Research* **106**(D16): 14 827–14 842.

Blöschl G, Sivapalan M. 1995. Scale issues in hydrological monitoring: a review. *Hydrological Processes* **9**: 251–290.

Brodzik MJ, Knowles K. 2002. EASE-Grid: a versatile set of equal-area projections and grids. In Goodchild M (ed.). *Discrete Global Grids*. National Center for Geographic Information and Analysis: Santa Barbara, CA, USA, http://www.ncgia.vcsb.edu/globalgrids-book/ease-grid/ Accessed 21 May 2002.

Broecker WS. 1997. Thermohaline circulation, the Achilles heel of our climate system: will man-made CO_2 upset the current balance? *Science* **278**: 1582–1588.

Brown J, Hinkel KM, Nelson FE. 2000. The Circumpolar Active Layer Monitoring (CALM) program. *Polar Geography* **24**(3): 165–258.

Bruland O, Maréchal D, Sand K, Killingtveit Å. 2001. Energy and water balance studies of a snow cover during snowmelt period at a high Arctic site. *Theoretical and Applied Climatology* **70**: 53–63.

Chapman WL, Walsh JE. 1993. Recent variations of sea ice and air temperature in high latitudes. *Bulletin of the American Meteorological Society* **74**(1): 33–47.

Federer CA, Lash D. 1978. *Brook: a hydrologic simulation model for eastern forests*. Technical report, University of New Hampshire Water Resources Research Center Research Report No. 19.

Fekete BM, Vörösmarty CJ, Grabs W. 1999. Global composite runoff fields based on observed river discharge and simulated water balance. Technical report, WMO Global Runoff Data Center Report #22, Koblenz, Germany.

Food and Agriculture Organization/UNESCO. 1995. Digital Soil Map of the World and Derived Properties, version 3.5, November, 1995. Original scale 1 : 5 000 000, UNESCO. Paris, France.

Global Soil Data Task. 2000. Global Soil Data Products CD-ROM (IGBP-DIS). CD-ROM. International Geosphere–Biosphere Programme, Data and Information System, Potsdam, Germany. Available from Oak Ridge National Laboratory Distributed Active Archive Center, Oak Ridge, Tennessee, USA. http://www.aaac.ornl.gov.

Groisman PY, Karl TR, Knight TW. 1994. Observed impact of snow cover on the heat balance and the rise of continental spring temperatures. *Science* **263**: 198–200.

Hamon WR. 1963. Computation of direct runoff amounts from storm rainfall. *International Association of Scientific Hydrology Publication* **63**: 52–62.

Hinzman LD, Kane DL. 1991. Snow hydrology of a headwater Arctic basin. 2. Conceptual analysis and computer modeling. *Water Resources Research* **27**(6): 1111–1121.

Hinzman LD, Kane DL. 1992. Potential response of an Arctic watershed during a period of global warming. *Journal of Geophysical Research* **97**: 2811–2820.

Holden JB. 1999. *A permafrost water balance model*. MS Thesis: University of New Hampshire (Department of Earth Sciences).

Holmes RM, Peterson BJ, Gordeev VV, Zhulidov AV, Maybeck M, Lammers RB, Vörösmarty CJ. 2000. Flux of nutrients from Russian rivers to the Arctic Ocean: can we establish a baseline against which to judge future change. *Water Resources Research* **36**(8): 2309–2320.

Jumikis AR. 1997. *Thermal Geotechnics*. Rutgers University Press: New Brunswick, NJ.

Kalnay E, Kanamitsu M, Kistler R, Collins W, Deaven D, Gandin L, Iredell M, Saha S, White G, Woolen J, Zhu Y, Chelliah M, Ebisuzaki W, Higgens W, Janowiak J, Ropelewski KC, Wang J, Leetma A, Reynolds R, Jenne R, Joseph D. 1996. The NCEP/NCAR 40-year reanalysis project. *Bulletin of the American Meteorological Society* **77**: 437–471.

Karl TR, Groisman PY, Knight RW Jr, Heim RR Jr. 1993. Recent variations of snow cover and snowfall in North America and their relation to precipitation and temperature variations. *Journal of Climate* **6**: 1327–1344.

Klene AE, Nelson FE, Shiklomanov NI, Hinkel KM. 2001. The N-factor in natural landscapes: variability of air and soil-surface temperatures, Kuparuk River basin, Alaska, U.S.A. Arctic. *Antarctic and Alpine Research* **33**(2): 140–148.
Lammers RB, Shiklomanov AI, Vörösmarty CJ, Fekete BM, Peterson BJ. 2001. Assessment of contemporary Arctic river runoff based on observational discharge records. *Journal of Geophysical Research* **106**(D4): 3321–3334.
Lunardini VJ. 1978. Theory of *N*-factor and correlation of data. In *Proceedings of the Third International Conference on Permafrost*, vol. 1. National Council of Canada: Ottawa; 40–46.
Lunardini VJ. 1981. *Heat Transfer in Cold Climates*. Van Nostrand Reinhold: New York.
Manabe S, Stouffer RJ, Spelman MJ, Bryan K. 1991. Transient responses of a coupled ocean–atmosphere model to gradual changes of atmospheric CO_2. Part I: annual mean response. *Journal of Climate* **4**: 785–817.
Maurer EP, O'Donnell GM, Lettenmaier DP, Roads JO. 2001. Evaluation of the land surface water budget in NCEP/NCAR and NCEP/DOE reanalysis using an off-line hydrological model. *Journal of Geophysical Research* **106**(D16): 17 841–17 862.
Mellilo JM, McGuire AD, Kicklighter DW, Moore B III, Vörösmarty CJ, Schloss AL. 1993. Global climate change and terrestrial net primary production. *Nature* **363**: 234–240.
Mintz Y, Walker GK. 1993. Global fields of soil moisture and land surface evapotranspiration derived from observed precipitation and surface air temperature. *Journal of Applied Meteorology* **32**: 1305–1334.
Nelson FE, Shiklomanov NI, Mueller GR. 1999. Variability of active-layer thickness at multiple spatial scale, north-central Alaska, U.S.A. *Arctic, Antarctic, and Alpine Research* **11**(2): 179–186.
Nelson FE, Shiklomanov NI, Mueller GR, Hinkel KM, Walker DA, Bockheim JG. 1997. Estimating active-layer thickness over a large region: Kuparuk River basin, Alaska, U.S.A. *Arctic and Alpine Research* **29**: 367–378.
Nicholls N, Gruza GV, Jouzel J, Karl TR, Ogallo LA, Parker DE. 1996. Observed climate variability and change. In *The IPCC Second Scientific Assessment*, Houghten JT, *et al*. (eds). Cambridge University Press: New York.
Nijssen B, O'Donnell GM, Lettenmaier DP, Lohmann D, Wood EF. 2001. Predicting the discharge of global rivers. *Journal of Climate* **14**: 3307–3323.
NSIDC. 1995. *The equal-area scalable grid*. Technical report, National Snow and Ice Data Center. http://nsidc.org/data/ease/index.html Accessed 21 May 2002.
Nyberg L, Stahli M, Mellander PE, Bishop KH. 2001. Soil frost effects on soil water and runoff dynamics along a boreal transect: 1. Field investigations. *Hydrological Processes* **15**: 909–926.
Oechel WC, Hastings SJ, Vourlitis G, Jenkins M, Riechers G, Grulke N. 1993. Recent change of Arctic tundra ecosystems from a net carbon sink to a source. *Nature* **361**: 520–523.
Pitman AJ, Slater AG, Desborough CE, Zhao M. 1999. Uncertainty in the simulation of runoff due to the parameterization of frozen soil moisture using the global soil moisture project methodology. *Journal of Geophysical Research* **104**(D14): 16 879–16 888.
Roads JO, Chen SC, Guetter A, Georgakakos K. 1994. Large-scale aspects of the United States hydrologic cycle. *Bulletin of the American Meteorological Society* **75**: 1589–1610.
Robock A, Vinnikov KY, Schlosser CA. 1995. Use of midlatitude soil moisture and meteorological observations to validate soil moisture simulations with biosphere bucket models. *Journal of Climate* **8**: 15–35.
Romanovsky VE, Osterkamp TE. 1995. Interannual variations of the thermal regime of the active layer and near-surface permafrost in northern Alaska. *Permafrost and Periglacial Processes* **6**: 313–335.
Schiller A, Mikolajewicz U, Voss R. 1997. The stability of the North Atlantic thermohaline circulation in a coupled ocean–atmosphere general circulation model. *Climate Dynamics* **13**: 325–347.
SEARCH SCC. 2001. *SEARCH: study of environmental Arctic change, science plan. Technical report, Seattle, Polar Science Center*, University of Washington. http://psc.apl.washington.edu/search Accessed 5 February 2002.
Serreze MC, Clark MP, Bromwich DA. 2002. Monitoring precipitation over the Arctic terrestrial drainage system: data requirements, shortcomings, and applications of atmospheric reanalysis. *Journal of Hydrometeorology* **4**(2): 287–407.
Serreze MC, Walsh JE, Chapin FS III, Osterkamp T, Dyurgerov M, Romanovsky V, Oechel WC, Morison J, Zhang T, Barry RG. 2000. Observation evidence of recent change in the northern high-latitude environment. *Climate Change* **46**: 159–207.
Shiklomanov AI, Lammers RB, Vörösmarty CJ. 2002. Widespread decline in hydrological monitoring threatens pan-Arctic research. *EOS Transactions, American Geophysical Union* **83**(2): 13–17.
Shiklomanov IA. 1998. *A comprehensive assessment of the freshwater resources of the world: assessment of water resources and availability in the world*. Technical report, WMO, UNDP, UNED, FAO, UNESCO, World Bank, WHO, UNIDO, SEI. WMO: Geneva.
Stahli M, Nyberg L, Mellander PE, Jamison PE, Bishop KH. 2001. Soil frost effects on soil water and runoff dynamics along a boreal transect: 1. Simulations. *Hydrological Processes* **15**: 927–941.
Uppala S, Gibson JK, Fiorino M, Hernandez A, Kallberg P, Li X, Onogi K, Saarinen S. 2000. ECMWF Second Generation Reanalysis. In *Proceedings of the Second WCRP International Conference on Reanalysis*. WMO/TD-No. 985; 9–13.
van Wijk WR, de Vries DA. 1963. Periodic temperature variations in homogeneous soil. In *Physics of Plant Environment*, van Wijk WR (ed.). North Holland: Amsterdam; 102–143.
Vörösmarty CJ, Federer CA, Schloss AL. 1998. Potential evapotranspiration functions compared on US watersheds: possible implications for global-scale water balance and terrestrial ecosystem modeling. *Journal of Hydrology* **207**: 147–169.
Vörösmarty CJ, Fekete BM, Maybeck M, Lammers RB. (2000a). Geomorphometric attributes of the global system of rivers at 30-min spatial resolution. *Journal of Hydrology* **237**: 17–39.
Vörösmarty CJ, Fekete BM, Maybeck M, Lammers RB. (2000b). Global system of rivers: its role in organizing continental land mass and defining land-to-ocean linkages. *Global Biogeochemical Cycles* **14**: 599–621.
Vörösmarty CJ, Hinzman LD, Peterson BJ, Bromwich DH, Hamilton LC, Morrison J, Romanovsky VE, Sturm M, Webb RS. 2001. *The hydrologic cycle and its role in Arctic and global environmental change: a rationale and strategy for synthesis study*. Technical report, Arctic Research Consortium of the U.S., Fairbanks, AK.

Vörösmarty CJ, Moore B III, Gildea MP, Peterson BJ, Melillo JM, Kicklighter DW, Raich J, Rastetter EB, Steudler P. 1989. Continental scale models of water balance and fluvial transport: an application to South America. *Global Biogeochemical Cycles* **3**(3): 241–265.
Vörösmarty CJ, Willmott CJ, Choudhury BJ, Schloss AL, Streans TK, Robeson SM, Dorman TJ. 1996. Analyzing the discharge regime of a large tropical river through remote sensing, ground-based climatic data and modeling. *Water Resources Research* **32**: 3137–3150.
Waelbroeck C, Monfray P, Oechel WC, Hastings S, Vourlitis G. 1997. The impact of permafrost thawing on the carbon dynamics of tundra. *Geophysical Research Letters* **24**: 229–232.
Walsh JE, Kattsov V, Portis D, Meleshko V. 1998. Arctic precipitation and evaporation. *Journal of Climate* **11**: 72–87.
Willmott CJ, Rowe CJ, Mintz Y. 1985. Climatology of the terrestrial seasonal water cycle. *Journal of Climate* **5**: 589–606.
Wolheim WM, Peterson BJ, Deegan LA, Hobbie JE, Hooker B, Bowden WB, Edwardson KJ, Arscott DB, Hershey AE, Finlay J. 2001. Influence of stream size on ammonium and suspended particulate nitrogen processing. *Limnology and Oceanography* **46**(1): 1–13.
Woo MK. 1998. Arctic snow cover information for hydrological investigations at various scales. *Nordic Hydrology* **29**: 245–266.
Yang D, Goodison BE, Ishida S, Benson CS. 1998. Adjustment of daily precipitation data at 10 stations in Alaska: application of World Meteorological Organization intercomparison results. *Water Resources Research* **34**(2): 241–256.
Zhang T, Osterkamp TE, Stamnes K. 1996. Some characteristics of the climate in northern Alaska. *Arctic and Alpine Research* **28**(4): 509–518.
Zhang T, Osterkamp TE, Stamnes K. 1997. Effects of climate on the active layer and permafrost on the North Slope of Alaska, U.S.A. *Permafrost and Periglacial Processes* **8**: 45–67.
Zhang T, Stamnes K. 1998. Impact of climatic factors on the active-layer and permafrost at Barrow, Alaska. *Permafrost and Periglacial Processes* **9**: 229–246.
Zhuang Q, Romanovsky VE, McGuire AD. 2001. Incorporation of a permafrost model into a large-scale ecosystem model: evaluation of temporal and spatial scaling issues in simulating soil thermal dynamics. *Journal of Geophysical Research* **106**(D24): 33 649–33 670.

